Arabian Journal of Chemistry (2017) **10**, 488–499

King Saud University

Arabian Journal of Chemistry

www.ksu.edu.sa
www.sciencedirect.com

ORIGINAL ARTICLE

Alpha-glucosidase and carbonic anhydrase inhibition studies of Pd(II)-hydrazide complexes

Qurrat-ul-Ain [a], Uzma Ashiq [a], Rifat Ara Jamal [a], Muhammad Saleem [b], Mohammad Mahroof-Tahir [c,d,*,1]

[a] *Department of Chemistry, University of Karachi, Karachi 75270, Pakistan*
[b] *H.E.J. Research Institute of Chemistry, International Center for Chemical and Biological Sciences, University of Karachi, Karachi 75270, Pakistan*
[c] *Department of Chemistry and Earth Sciences, PO Box 2713, Qatar University, Doha, Qatar*
[d] *Department of Chemistry and Biochemistry, St. Cloud State University, St. Cloud, MN 56304, USA*

Received 26 September 2014; accepted 27 February 2015
Available online 6 March 2015

KEYWORDS

Pd(II) complexes;
Hydrazide;
α-Glucosidase;
Carbonic anhydrase;
Enzyme

Abstract This study focused on the synthesis and characterization of hydrazide ligands and their respective Pd(II) complexes and used high throughput screening to determine their α-glucosidase and carbonic anhydrase II enzyme inhibition activities. The physical, analytical (elemental analyses for C, H, N and Pd) and spectral (FT-IR, ^{1}H NMR, ^{13}C NMR, EI-mass) techniques utilized during characterization revealed the formation of square planar, neutral and 1:2 Pd(II)-hydrazide complexes with the general formula $[PdL_2Cl_2]$. In these Pd(II) complexes, the hydrazide ligands are monodentate; the terminal nitrogen is the donor atom. The uncoordinated hydrazide ligands were inactive against both α-glucosidase and carbonic anhydrase II enzymes; however, the respective Pd(II)-hydrazide complexes were approximately 300 times more potent α-glucosidase inhibitors than the standard compound, 1-deoxynojirimycin (DNJ). Some of the Pd(II) complexes also demonstrated potential carbonic anhydrase (CA) inhibition properties comparable to the standard compound, acetazolamide (ACZ).

* Corresponding author at: Department of Chemistry and Biochemistry, St. Cloud State University, St. Cloud, MN 56304, USA. Tel.: +1 320 308 3198; fax: +1 320 308 6041.
E-mail addresses: mmahroof@qu.edu.qa, mmahroof@stcloudstate.edu (M. Mahroof-Tahir).
[1] Tel.: +974 6680 4352.
Peer review under responsibility of King Saud University.

ELSEVIER Production and hosting by Elsevier

1. Introduction

Diabetes mellitus (DM) is a well-known, progressive endocrine disorder associated with increased morbidity and mortality, as well as high health care costs. There were approximately 171 million cases of DM in 2000, and this number is expected to more than double over the next 25 years, reaching 366 million by 2030 (Funke and Melzig, 2006; Si et al., 2010). This increasing trend has become a serious worldwide medical concern that stimulates the search for new therapeutic agents.

http://dx.doi.org/10.1016/j.arabjc.2015.02.024
1878-5352

DM is characterized by hyperglycemia and alterations in carbohydrate, protein, and lipid metabolisms, caused by defects in insulin production or action (Jaiswal et al., 2012). Postprandial hyperglycemia is a prominent defect that occurs early in diabetes (Carroll et al., 2003) and may lead to various secondary complications, including elevated risk for cardiovascular diseases (Slama et al., 2006), atherosclerosis, cataracts, retinopathy, neuropathy, nephropathy and impaired wound healing (Atta-ur-Rahman et al., 2007). Ingesting a carbohydrate-rich diet triggers elevated blood glucose levels due to the rapid absorption of carbohydrates, which is aided by glycoside hydrolases, such as alpha-glucosidase (EC 3.2.1.20); this enzyme is present in the epithelial mucosa of the small intestine and cleaves the glycosidic bonds in complex carbohydrates to release absorbable monosaccharides (Chiba, 1997). One therapeutic approach for treating diabetes involves controlling postprandial hyperglycemia by inhibiting the alpha-glucosidase in the digestive tract, delaying and prolonging the overall carbohydrate digestion time. Slowing carbohydrate digestion should reduce the rate of glucose absorption and consequently prevent spikes in the postprandial blood glucose and insulin levels (Kim et al., 2008; Chiasson and Rabasa Lhoret, 2004). Using α-glucosidase inhibitors has become a promising therapeutic strategy for reducing the risks of diabetes and other carbohydrate-mediated diseases, including hyperlipoproteinemia and obesity (Franco et al., 2002; Braun et al., 1995; Dwek et al., 2002; Sou et al., 2001; Mehta et al., 1998; Karpas et al., 1988; Zitzmann et al., 1999; Truscheit et al., 1981; Madariaga et al., 1988; Lajolo et al., 1984; McCulloch et al., 1983).

Carbonic anhydrases (CA, EC 4.2.1.1) are zinc-containing metalloproteins. These enzymes reversibly catalyze the conversion of carbon dioxide to bicarbonate ions (Tripp et al., 2001). CAs form a group of catalytic enzymes that are vital for many physiological processes, including respiration and carbon dioxide/bicarbonate transport between the lungs and metabolizing tissues. These enzymes are also involved in important biological and patho-physiological functions, such as tumorigenicity, gluconeogenesis, bone resorption, lipogenesis, calcification, ureagenesis and electrolyte secretion, as well as carbon dioxide and pH homeostasis (Ho et al., 2003). This enzymatic family contains potential therapeutic targets for many diseases. Currently, CA inhibitors are first line treatments for neurological disorders, osteoporosis, glaucoma, cancer and obesity, as well as gastric and duodenal ulcers; CA inhibitors may also act as diuretics and antiepileptics (Supuran et al., 2004, 2003; Supuran and Scozzafava, 2000). CA inhibitors have the ability to dilate retinal capillaries and suppress capillary blockage (Mirshafiey and Boghozian, 2011).

Several metal ions and their complexes exhibit diverse biological activities, including antidiabetic effects (Schwarz and Mertz, 1959; Rubenstein et al., 1962; Coulston and Dandona, 1980; Heyliger et al., 1985; Sakurai et al., 1990; Yoshikawa et al., 2000; Ueda et al., 2005; Ashiq et al., 2008), as well as phosphodiesterase (Ashiq et al., 2009), urease (Ara et al., 2007) and carbonic anhydrase (Scozzafava and Supuran, 1997; Supuran et al., 1997) inhibition; metal ions and complexes may also display antifungal (Maqsood et al., 2006) and antioxidant (Ashiq et al., 2008, 2009; Qurrat-ul-Ain et al., 2013) properties. However, enzyme inhibition studies on Pd(II) complexes are rare. This study evaluates the alpha-glucosidase inhibition potential of Pd(II) hydrazide complexes, which could lead to the improvement of postprandial hyperglycemia and identification of new carbonic anhydrase inhibitors to control the effects of cancer, glaucoma and neurological disorders.

2. Materials and methods

2.1. Chemistry

All the chemicals were of reagent grade, purchased from BDH, Merck or Sigma–Aldrich and used without further purification. A Shimadzu 460 IR spectrophotometer was employed to record FT-IR spectra at 400–4000 cm^{-1} on KBr disks. ^{1}H NMR and ^{13}C NMR spectra in freshly prepared DMSO solutions were obtained from a Bruker 300 spectrometer at 300 or 400 MHz using TMS as internal standard. EI-mass data of ligands were collected from a Finnigan MAT 311-A apparatus. A Sherwood MSB Mk1 magnetic susceptibility balance was utilized to measure effective magnetic moments of powdered complexes at room temperature using sealed-off $MnCl_2$ solution as calibrant. CHN (elemental) analysis was carried out on a Perkin Elmer 2400 series II CHN/ S analyzer. Pd contents in complexes were analyzed by EDTA titration using sodium nitrite as a selective masking agent in the presence of xylenol orange indicator (Muralidhara et al., 1995). A Hanna (HI-8633) conductivity meter was used for conductance measurement. The carbonic anhydrase II was purchased from Sigma Aldrich and substrate 4-nitrophenyl acetate from MP Bio chemical company. HEPES buffer was obtained from DOJINDO, Tris-(hydroxymethyl)-aminomethane (reagent grade) from Scharlau and DMSO from Fischer Scientific chemical company. The α-glucosidase enzyme (purified from *Saccharomyces Cerevisiae*) and all other chemicals required for α-glucosidase inhibition assay were also purchased from Sigma Aldrich. IC_{50} values were calculated by using EZ-fit enzyme kinetics software (USA).

2.1.1. General procedure for the synthesis of the hydrazide ligands

Hydrazide ligands were synthesized from corresponding esters (Scheme 1). The ethyl or methyl esters were first obtained on

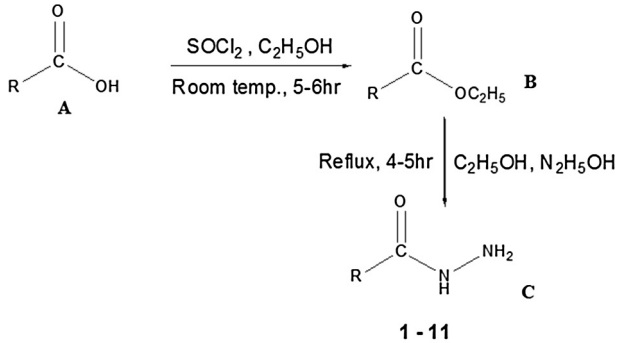

1	R = 2-F-C_6H_4	6	R = 2-OCH_3-C_6H_4
2	R = 3-F-C_6H_4	7	R = 3-OCH_3-C_6H_4
3	R = 4-F-C_6H_4	8	R = 4-OCH_3-C_6H_4
4	R = NH-C_6H_5	9	R = 2-Cl-C_6H_4
5	R = CH_2-C_6H_5	10	R = 3-Cl-C_6H_4
		11	R = 4-Cl-C_6H_4

Scheme 1 General procedure for the synthesis of ligands **1–11**.

stirring the substituted carboxylic acids with thionyl chloride in ethanol for 5–6 h followed by extraction in chloroform. After solvent evaporation, the esters (66 mmol) and hydrazine hydrate (330 mmol) were refluxed in 75 ml ethanol for 4–5 h. The solvent from resulting mixture was evaporated on rotary evaporator to get a colorless solid product. The hydrazide product was finally washed and dried in air. The relevant spectral and elemental data are given below.

*2.1.1.1. 2-Fluorobenzohydrazide (**1**).* Colorless solid. Anal. Calcd. for $C_7H_7N_2OF$ (FW = 154 $gmol^{-1}$): C, 54.54; H, 4.54; N, 18.18%. Found: C, 54.58; H, 4.56; N, 18.15%. FTIR (KBr cm^{-1}): 1674 (C═O), 3288, 3206 (NH_2 stretch.), 3037 (NH), 1616 (NH_2 bend.), 1567 (C═C), 1343 (C—N), 1228 (C—O), 1098 (N—N). ^{1}H NMR (400 MHz, DMSO): δ(ppm) = 9.49 (s, 1H, NH), 7.60 (dd, 1H, *J* = 5.5 Hz, *J* = 2.4 Hz, H-6), 7.56 (dt, 1H, *J* = 6.8 Hz, *J* = 2.0 Hz, H-4), 7.50 (dt, 1H, *J* = 6.6 Hz, H-3), 7.26 (dd, 1H, *J* = 8.0 Hz, *J* = 2.8 Hz, H-5), 4.52 (s, 2H, NH_2). ^{13}C NMR (400 MHz, DMSO): δ(ppm) = 163.27 (C═O), 115.91–160.27 (Ar—C). EI MS: 154 (19, M^+), 124 (8), 123 (100), 95 (35), 75 (7).

*2.1.1.2. 3-Fluorobenzohydrazide (**2**).* Colorless solid. Anal. Calcd. for $C_7H_7N_2OF$ (FW = 154 $gmol^{-1}$): C, 54.54; H, 4.54; N, 18.18%. Found: C, 54.57; H, 4.53; N, 18.11%. FTIR (KBr cm^{-1}): 1663 (C═O), 3300, 3219 (NH_2 stretch.), 3026 (NH), 1620 (NH_2 bend.), 1585 (C═C), 1349 (C—N), 1232 (C—O), 1009 (N—N). ^{1}H NMR (400 MHz, DMSO): δ(ppm) = 9.85 (s, 1H, NH), 7.67 (d, 1H, *J* = 8.0 Hz, H-6), 7.59 (dd, 1H, *J* = 10.4 Hz, *J* = 2.0 Hz, H-2), 7.49 (dd, 1H, *J* = 6.0 Hz, *J* = 2.0 Hz, H-5), 7.34 (dt, 1H, *J* = 8.8 Hz, *J* = 2.8 Hz, H-4), 4.51 (s, 2H, NH_2). ^{13}C NMR (400 MHz, DMSO): δ(ppm) = 164.38 (C═O), 113.51–163.06 (Ar—C). EI MS: 154 (47, M^+), 124 (15), 123 (100), 95 (95), 75 (47), 57 (4), 51 (13).

*2.1.1.3. 4-Fluorobenzohydrazide (**3**).* Colorless solid. Anal. Calcd. for $C_7H_7N_2OF$ (FW = 154 $gmol^{-1}$): C, 54.54; H, 4.54; N, 18.18%. Found: C, 54.60; H, 4.57; N, 18.20%. FTIR (KBr cm^{-1}): 1661 (C═O), 3303, 3223 (NH_2 stretch.), 3023 (NH), 1620 (NH_2 bend.), 1564 (C═C), 1350 (C—N), 1243 (C—O), 997 (N—N). ^{1}H NMR (300 MHz, DMSO): δ(ppm) = 9.75 (s, 1H, NH), 7.87 (dd, 2H, *J* = 4.8 Hz, *J* = 3.9 Hz, H-2/H-6), 7.26 (dt, 2H, *J* = 8.1 Hz, *J* = 2.1 Hz, H-3/H-5), 4.47 (s, 2H, NH_2). ^{13}C NMR (400 MHz, DMSO): δ(ppm) = 164.40 (C═O), 114.53–164.28 (Ar—C). EI MS: 154 154 (9, M^+), 124 (8), 123 (100), 95 (93), 75 (35), 57 (4), 51 (11).

*2.1.1.4. 4-Phenylsemicarbazide (**4**).* Colorless solid. Anal. Calcd. for $C_7H_9N_3O$ (FW = 151 $gmol^{-1}$): C, 55.62; H, 5.96; N, 27.81%. Found: C, 55.64; H, 5.98; N, 27.86%. FTIR (KBr cm^{-1}): 1687 (C═O), 3362, 3260 (NH_2 stretch.), 3094 (NH), 1595 (NH_2 bend.), 1540 (C═C), 1302 (C—N), 1226 (C—O), 925 (N—N). ^{1}H NMR (400 MHz, DMSO): δ(ppm) = 8.57 (s, 1H, NH), 7.49 (d, 2H, *J* = 7.8 Hz, H-2/H-6), 7.33 (s, 1H, phNHCO), 7.21 (t, 2H, *J* = 7.8 Hz, H-3/H-5), 6.90 (t, 1H, *J* = 7.2 Hz, H-4), 4.31 (s, 2H, NH_2). ^{13}C NMR (400 MHz, DMSO): δ(ppm) = 157.28 (C═O), 118.05–139.87 (Ar—C). EI MS: 151 (61, M^+), 120 (15), 119 (25), 92 (41), 77 (100), 65 (49), 51 (35).

*2.1.1.5. 2-Phenylacetohydrazide (**5**).* Colorless solid. Anal. Calcd. for $C_8H_{10}N_2O$ (FW = 150 $gmol^{-1}$): C, 64.76; H, 6.66; N, 18.66%. Found: C, 64.73; H, 6.68; N, 18.67%. FTIR (KBr cm^{-1}): 1643 (C═O), 3295, 3200 (NH_2 stretch.), 3030 (NH), 1566 (NH_2 bend.), 1529 (C═C), 1352 (C—N), 1265 (C—O), 997 (N—N). ^{1}H NMR (400 MHz, DMSO): δ(ppm) = 9.19 (s, 1H, NH), 7.23–7.28 (m, 5H, H-2/H-3/H-4/H-5/H-6), 3.56 (s, 2H, phCH_2CO), 4.19 (s, 2H, NH_2). ^{13}C NMR (400 MHz, DMSO): δ(ppm) = 168.94 (C═O), 136.19 (phCH_2), 125.74–128.34 (Ar—C). EI MS: 150 (36, M^+), 137 (2), 120 (2), 118 (51), 106 (5), 91 (100), 77 (14), 65 (51), 51 (54).

The analytical data of 2-Methoxybenzohydrazide (**6**), 3-Methoxybenzohydrazide (**7**), 4-Methoxybenzohydrazide (**8**) were reported previously (Qurrat-ul-Ain et al., 2013), whereas 2-Chlorobenzohydrazide (**9**), 3-Chlorobenzohydrazide (**10**) and 4-Chlorobenzohydrazide (**11**) will be reported elsewhere.

2.1.2. General procedure for the synthesis of the palladium(II)-hydrazide complexes

Two complexes (**1b** and **2b)** were synthesized in water, while remaining complexes (**3b–5b)** were prepared in acetonitrile. 30 ml solution of palladium(II) chloride (1 mmol) in acetonitrile or water containing one drop of concentrated HCl was mixed slowly with 30 ml solution of hydrazide (2 mmol) in the same solvent. The yellow precipitates started forming immediately, which were kept on stirring for about 3 h at room temperature. The yellow solid complex was then separated, washed with water or acetonitrile and finally allowed to dry in air. The physical, elemental and spectral data of complexes **1b–5b** are presented below.

*2.1.2.1. Dichlorobis(2-fluorobenzohydrazide)palladium(II) [Pd(2-fbh)$_2$Cl$_2$] (**1b**).* Yellow solid. Anal. Calcd. for $C_{14}H_{14}N_4O_2F_2Cl_2Pd$ (FW = 485.70 $gmol^{-1}$): C, 34.60; H, 2.88; N, 11.54; Pd, 21.92%. Found: C, 33.52; H, 2.13; N, 10.13; Pd, 22.01%. FTIR (KBr cm^{-1}): 1666 (C═O), 3372 (NH_2 stretch.), 3208 (NH), 1615 (NH_2 bend.), 1526 (C═C), 1309 (C—N), 1212 (C—O), 1099 (N—N). ^{1}H NMR (400 MHz, DMSO): δ(ppm) = 9.58 (s, 1H, NH), 7.24–7.72 (Aromatic-H), 4.95 (s, 2H, NH_2). ^{13}C NMR (400 MHz, DMSO): δ(ppm) = 160.59 (C═O), 115.61–159.72 (Ar—C). Molar conductivity (DMSO): 5.12 Ω^{-1} cm^2 mol^{-1}. Effective magnetic moment: 0.198 B.M. Yield: 78.50%.

*2.1.2.2. Dichlorobis(3-fluorobenzohydrazide)palladium(II) [Pd(3-fbh)$_2$Cl$_2$] (**2b**).* Yellow solid. Anal. Calcd. for $C_{14}H_{14}N_4O_2F_2Cl_2Pd$ (FW = 485.70 $gmol^{-1}$): C, 34.60; H, 2.88; N, 11.54; Pd, 21.92%. Found: C, 33.94; H, 2.01; N, 10.88; Pd, 21.25%. FTIR (KBr cm^{-1}): 1655 (C═O), 3270, 3196 (NH_2 stretch.), 3100 (NH), 1604 (NH_2 bend.), 1585 (C═C), 1329 (C—N), 1215 (C—O), 948 (N—N). ^{1}H NMR (400 MHz, DMSO): δ(ppm) = 9.99 (s, 1H, NH), 7.36–7.68 (Aromatic-H), 5.29 (s, 2H, NH_2). ^{13}C NMR (400 MHz, DMSO): δ(ppm) = 164.44 (C═O), 113.61–163.48 (Ar—C). Molar conductivity (DMSO): 9.09 Ω^{-1} cm^2 mol^{-1}. Effective magnetic moment: 0.219 B.M. Yield: 84.15%.

*2.1.2.3. Dichlorobis(4-fluorobenzohydrazide)palladium(II) [Pd(4-fbh)$_2$Cl$_2$] (**3b**).* Yellow solid. Anal. Calcd. for $C_{14}H_{14}N_4O_2F_2Cl_2Pd$ (FW = 485.70 $gmol^{-1}$): C, 34.60; H, 2.88; N, 11.54; Pd, 21.92%. Found: C, 34.32; H, 2.56; N,

11.45; Pd, 20.85%. FTIR (KBr cm^{-1}): 1604 (C═O), 3310, 3203 (NH_2 stretch.), 3106 (NH), 1604 (NH_2 bend.), 1535 (C═C), 1326 (C—N), 1238 (C—O), 905 (N—N). ^1H NMR (400 MHz, DMSO): δ(ppm) = 9.94 (s, 1H, NH), 7.23–7.88 (Aromatic-H), 5.49 (s, 2H, NH_2). ^{13}C NMR (400 MHz, DMSO): δ(ppm) = 164.33 (C═O), 114.64–162.63 (Ar—C). Molar conductivity (DMSO): 2.08 Ω^{-1} cm^2 mol^{-1}. Effective magnetic moment: 0.147 B.M. Yield: 88.90%.

*2.1.2.4. Dichlorobis(4-phenylsemicarbazide)palladium(II) [Pd(4-psc)$_2$Cl$_2$] (**4b**).* Yellow solid. Anal. Calcd. for $C_{14}H_{18}N_6O_2Cl_2Pd$ (FW = 479.76 $gmol^{-1}$): C, 35.01; H, 3.75; N, 17.52; Pd, 22.18%. Found: C, 35.00; H, 3.50; N, 16.95; Pd, 21.17%. FTIR (KBr cm^{-1}): 1681 (C═O), 3450, 3339 (NH_2 stretch.), 3197 (NH), 1643 (NH_2 bend.), 1603 (C═C), 1320 (C—N), 1257 (C—O), 1030 (N—N). ^1H NMR (400 MHz, DMSO): δ(ppm) = 9.26 (s, 1H, NH), 6.99–7.82 (Aromatic-H), 7.35 (s, 1H, phNHCO), 6.47 (s, 2H, NH_2). ^{13}C NMR (400 MHz, DMSO): δ(ppm) = 154.33 (C═O), 117.93–138.99 (Ar—C). Molar conductivity (DMSO): 12.42 Ω^{-1} cm^2 mol^{-1}. Effective magnetic moment: 0.132 B.M. Yield: 88.90%.

*2.1.2.5. Dichlorobis(2-Phenylacetohydrazide)palladium(II) [Pd(2-pah)$_2$Cl$_2$] (**5b**).* Yellow solid. Anal. Calcd. for $C_{16}H_{20}N_4O_2Cl_2Pd$ (FW = 477.78 $gmol^{-1}$): C, 40.21; H, 4.19; N, 11.73; Pd, 22.29%. Found: C, 40.38; H, 3.78; N, 11.77; Pd, 21.97%. FTIR (KBr cm^{-1}): 1650 (C═O), 3322, 3198 (NH_2 stretch.), 3116 (NH), 1602 (NH_2 bend.), 1547 (C═C), 1357 (C—N), 1268 (C—O), 1077 (N—N). ^1H NMR (400 MHz, DMSO): δ(ppm) = 9.80 (s, 1H, NH), m7.26 (Aromatic-H), 6.63 (s, 2H, NH_2), 3.57 (s, 1H, phCH_2CO). ^{13}C NMR (400 MHz, DMSO): δ(ppm) = 168.95 (C═O), 136.19 (phCH_2), 126.00–128.57 (Ar—C). Molar conductivity (DMSO): 3.90 Ω^{-1} cm^2 mol^{-1}. Effective magnetic moment: 0.153 B.M. Yield: 82.25%.

2.2. α-Glucosidase inhibition

The in vitro α-glucosidase inhibition assay was performed by spectrophotometric method described by Dewi et al., 2007 with slight modifications, involving hydrolysis of substrate *p*-nitrophenyl α-D-glucopyranoside according to Scheme 2 (Srianta et al., 2013).

The enzyme α-glucosidase was dissolved in a buffer of pH 6.8 containing 3 mM sodium phosphate and 6 mM NaCl. In a 96-well plate reader, a reaction mixture comprising 20 µl of varying concentrations (0.02–10 µM) of sample dissolved in DMSO (4.6% final concentration) and 100 µl of alpha-glucosidase (1 U/ml) was pre-incubated for 5 min at 37 °C, and then 260 µl of 0.5 mM *p*-nitrophenyl α-D-glucopyranoside was added to the mixture. After further incubation at 37 °C for 30 min, the reaction was terminated by adding 70 µl of sodium carbonate (0.1 M). The yellow color produced (due to *p*-nitrophenol formation) was quantitated by measuring the absorbance at 400 nm. The standard 1-deoxynojirimycin was used as a positive control. The % inhibition was obtained using the formula: % inhibition = [{Absorbance$_{(control)}$ − Absorbance$_{(sample)}$}/Absorbance$_{(control)}$] * 100. Each experiment was performed in triplicates. The IC_{50} (i.e., the concentration of sample inhibiting 50% of alpha-glucosidase activity under the stated assay conditions) data of Pd(II) hydrazide complexes, metal salt and standard are given in Table 1.

2.3. Carbonic anhydrase inhibition

In this assay, colorless 4-nitrophenyl acetate (4-NPA) is hydrolyzed to 4-nitrophenol and CO_2, and the reaction is followed by measuring the formation of 4-nitrophenol, a yellow colored compound (Pocker and Meany, 1967).

The assay was carried out at 25 °C in 20 mM HEPES-Tris buffer of pH 7.4. Each sample tube comprised 140 µl of HEPES-Tris buffer solution, 20 µl of fresh enzyme solution (0.1 mg/ml in deionized water) of purified bovine erythrocyte CA-II and 20 µl of test compound in DMSO (10% final concentration) at varying concentrations (3–500 µM). The enzyme and inhibitor together in mixture solution were preincubated for 15 min at room temperature to allow the formation of EI complex. After incubation, the reaction with substrate was initiated by adding 20 µl ethanolic solution (0.7 mM) of 4-NPA. It was followed by continuous measurement of amount of product formed at 400 nm for 30 min at 1 min interval in 96-well flat bottom plates, using ELISA Reader SPECTRA-Max 340 spectrophotometer, Molecular Devices (USA). The activity of control (in the absence of inhibitor) was taken as 100%. The measurements were taken in triplicates at each used concentration (Shank et al., 2005; Arslan, 2001).

2.3.1. Enzyme kinetic studies

To determine the kinetic parameters, the substrate (4-nitrophenyl acetate) was used at four different concentrations (0.18–1.4 mM). The solution of potential inhibitors, identified by low IC_{50} values, was added to the reaction medium at various concentrations under assay conditions stated above, resulting in at least three different fixed concentrations (3–50 µM) of inhibitors (Pocker and Meany, 1967).

A Lineweaver–Burk plot was generated to identify the type of inhibition. The Michaelis–Menten constant (K_m) value was obtained from Lineweaver–Burk plot between reciprocal of the substrate concentration (1/[*S*]) and reciprocal of enzyme rate

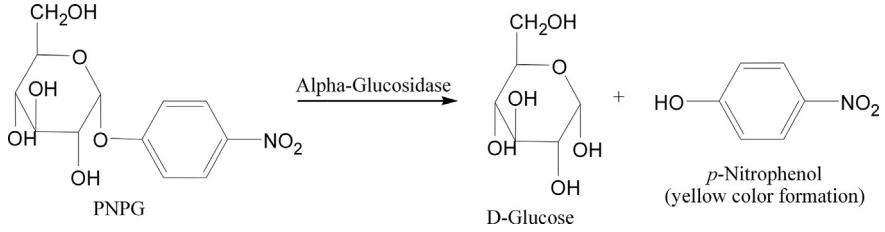

Scheme 2 Mechanism of hydrolysis of p-nitrophenyl alpha-D-glucopyranoside (pNPG) by α-glucosidase.

$(1/V)$ over different inhibitor concentrations. To determine inhibition constant (K_i), a secondary re-plot of the inhibitor concentration ([*I*]) versus the slope (i.e., K_m/V_{max}) was constructed. The Dixon plot between [*I*] and $1/V$ was drawn to further confirm the K_i value and the type of inhibition of CA II (Cornish-Bowden, 1974).

2.3.2. Statistical analysis

Grafit 7.0 version was used to determine the kinetic parameters. The software was purchased from Erithacus Software Ltd. Wilmington House, High Street, East Grinstead, West Sussex RH19 3AU, UK.

3. Results and discussion

3.1. Synthesis and physicochemical properties

The synthesis of hydrazide ligands **1–11** was carried out according to Scheme 1; these molecules were subsequently complexed with Pd(II) to synthesize respective complexes (**1b–11b**). Five ligands (**1–5**) were characterized spectroscopically (IR, ^{1}H NMR, ^{13}C NMR, EI-mass) and micro-analytically (CHN), as presented in the experimental section. The structures of complexes **1b–5b** are depicted in Fig. 1 and were assigned based on their physical, chemical and spectral measurements presented in experimental part; the data for **6b–8b** have been reported previously (Qurrat-ul-Ain et al., 2013), and the data for **9b–11b** will be reported elsewhere. All of the Pd(II) complexes were amorphous, non-hygroscopic, yellow-colored, and fairly stable at room temperature. The complexes were highly soluble in coordinating solvents, such as DMF, DMSO and THF; however, the complexes revealed poor solubility in other solvents, such as water, acetone, methanol and ethanol.

The sharp, well-defined signals for the Pd(II) complexes in the NMR spectra reveal the diamagnetic nature of different complexes which is also supported by low magnetic moments (0.132–0.219 BM). Based on these studies we tentatively propose a square planar geometry (Fig. 1) for these complexes (Blanchard et al., 2005). All of the ligands exhibited monodentate behavior to form 1:2 metal–ligand complexes with Pd(II). Two chloride ions were also present within the coordination sphere. Ligands **1–5** coordinate to the metal via their terminal nitrogen. The complexes are likely to be the trans isomers

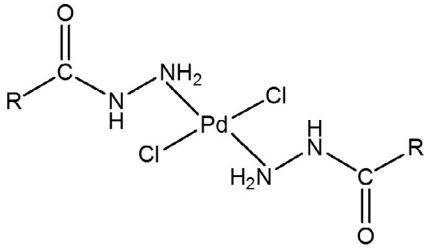

1b R = 2-F-C_6H_4
2b R = 3-F-C_6H_4
3b R = 4-F-C_6H_4
4b R = NH- C_6H_5
5b R = CH_2-C_6H_5

Figure 1 Structures of palladium(II) complexes.

because this configuration minimizes the steric hindrance between the hydrazide ligands (Kealey et al., 2007). Furthermore, the ligands ensure that the trans isomers remain separate by minimizing any possible cis–trans isomerism caused by steric effects (Abu-Surrah et al., 2002). The insolubility of Pd(II)-hydrazide complexes in polar solvents (water, methanol, etc.) also supports the trans nature of complexes. The trans complexes, being symmetrical, are non-polar, and thus they have poor solubility in polar solvents (Ebbing and Steven, 2010).

Freshly prepared DMSO solutions of complexes **1b–5b** possessed low ranging molar conductivities (2.08–12.42 Ω^{-1} cm^2 mol^{-1}), suggesting they are non-electrolytic (Teotia et al., 1973). The complexes were assumed to have the general formula $[PdL_2Cl_2]$, as indicated by the CHN and Pd contents reported in experimental section.

3.2. Spectroscopy

3.2.1. IR spectroscopy

The IR vibrational data for hydrazide ligands **1–5** and their palladium(II) complexes **1b–5b** are provided in experimental section. A pair of intense peaks at 3200 and 3362 cm^{-1} was exhibited by all ligands, and these peaks are attributed to the N-H asymmetric and symmetric stretching modes of the terminal hydrazinic amino group (Singh et al., 2005). After complexation to form **1b–5b**, these bands were shifted significantly toward higher or lower wavenumbers relative to the free ligands. Therefore, the terminal amino nitrogen coordinates with palladium(II) in ligands **1–5** (Adeoye et al., 2007; Abd El Wahed et al., 2004).

The strong carbonyl stretching absorption band occurs at 1665 ± 22 cm^{-1} in the ligands; this band is near the amide carbonyl absorptions (1655 ± 15 cm^{-1}) (Singh et al., 2005; Adeoye et al., 2007). Each of the ligands (**1–5**) exhibited only a small decrease in the carbonyl absorption band after complexation, suggesting that coordination did not occur through the carbonyl oxygen. The bands assigned to the NH_2 bending, as well as the C—N, C—O, N—N, and the aromatic C=C stretching (Ziolo et al., 1971; Basu et al., 1999; Piotr et al., 2005; Sharma et al., 2009; Pradeep et al., 2008; Chohan and Praveen, 1999) are also reported in experimental section.

The hydrazinic imino group in the ligands also generated a sharp band at 3058 ± 35 cm^{-1} (Singh et al., 2005) that shifts only slightly after complexation because the palladium(II) coordinates with the neighboring amino group. The IR vibrational data suggested that the ligands were monodentate. In complexes **1b–5b**, the coordination site might be the terminal hydrazinic amino nitrogen.

The sharp bands appeared in the FT-IR spectra of Pd(II)-hydrazide complexes advocate their trans geometry (Mukherjee et al., 2011). The vibrational spectra revealed a single sharp band at 530–540 cm^{-1} corresponding to Pd-N symmetric stretching for Pd(II)-hydrazide complexes, which further confirms the trans geometry of complexes (Lubna et al., 2014; Mukherjee et al., 2011). The sharp and well defined –NH stretching bands are sometimes assigned to hydrogen bonded –NH groups (Pavia et al., 2001). In present case, it is assumed that the intramolecular hydrogen bonding may exist between –NH and fluoro/carbonyl groups in the same hydrazide ligand (orienting trans to other hydrazide) instead of

Table 1 α-Glucosidase inhibition activity of palladium(II) complexes **1b–11b**.

Compound	IC_{50} (μM)	Compound	IC_{50} (μM)
1b	0.20 ± 0.005	**8b**	0.63 ± 0.002
2b	0.58 ± 0.002	**9b**	0.40 ± 0.001
3b	0.09 ± 0.001	**10b**	1.11 ± 0.008
4b	0.79 ± 0.008	**11b**	1.06 ± 0.005
5b	1.20 ± 0.009	$PdCl_2$	0.45 ± 0.001
6b	0.85 ± 0.005	DNJ	300 ± 1.72
7b	1.12 ± 0.007	–	–

DNJ = 1-Deoxynojirimycin, the standard inhibitor of α-glucosidase.

hydrogen bonding between two adjacent hydrazides in cis configuration.

3.2.2. *^{1}H NMR spectroscopy*

The ^{1}H NMR spectral data of the hydrazide ligands (**1–5**) and their complexes (**1b–5b**) are presented in experimental section. The signal assigned to the terminal amino protons appeared between 4.19 and 4.52 ppm for the ligands and shifted downfield after complexation to form **1b–5b**, indicating that the amino nitrogen coordinates with Pd(II) in these complexes (Abd El Wahed et al., 2004). The singlet at 8.57–9.99 ppm for the ligands and their complexes was attributed to the imino NH group, suggesting that the ligands exist in their keto (protonated) form in DMSO even after complexation and therefore cannot directly coordinate to Pd(II) via the imino NH (Sunirban and Samudranil, 2006). The negligible shift after complexation for the imino NH signal for all of the ligands further supports that the imino NH group is unavailable for coordination. Therefore, the ^{1}H NMR spectral results agree with the IR results. The aromatic proton NMR signals for ligands **1–5** validate the 6.89–7.91 ppm chemical shifts (Abdul et al., 2011; Pradeep et al., 2008). In the complexes, the aromatic protons' resonances generally have higher chemical shift values because there is increased conjugation after complexation (Ballhausen and Gray, 1962).

3.2.3. *^{13}C NMR spectroscopy*

The ^{13}C NMR spectral data for free ligands and respective Pd(II) complexes are displayed in experimental section and validate the bonding modes evident in the IR and ^{1}H NMR spectral studies discussed above. The number of carbon peaks observed for the ligands and their respective complexes matches the expected values. The aromatic carbon signals for the ligands are within 113.51–164.28 ppm (Chohan and Hanif, 2011) and shift slightly after complexation due to changes in conjugation. The carbonyl carbon signals appear at the furthest downfield position (Mishra and Soni, 2008) within 157.28–168.94 ppm for ligands **1–5** (Kucukguzel et al., 2003). The position of the carbonyl signal remained almost same for the complexes (**1b–5b**), clearly excluding the possibility of carbonyl coordination in these complexes.

The electron density at the reactive site on each ligand molecule depends on the polar properties of its substituents when all other factors remain constant (Zhdanov and Minkin, 1966). This aspect might explain the variable coordination behavior exhibited by various hydrazides toward Pd(II). The amino nitrogen is a soft base and a stronger σ-donor relative to the carbonyl oxygen (Sunirban and Samudranil, 2006). Therefore, because Pd(II) is a soft acid, it usually prefers nitrogen instead of oxygen coordination, as observed in complexes **1b–5b**. However, the carbonyl group is a relatively poor σ-donor and a hard base; this functionality might be a good π-electron acceptor if the electron density is decreased to strengthen the metal–oxygen bond via π-back bonding (Kuznetsov et al., 2006). Consequently, the hydrazides' electronic and steric properties could be used to tune their bonding mode toward the Pd(II) center.

3.3. *α-Glucosidase inhibition*

The α-glucosidase inhibition activity data are reported in Table 1, representing the IC_{50} values for Pd(II)-hydrazide

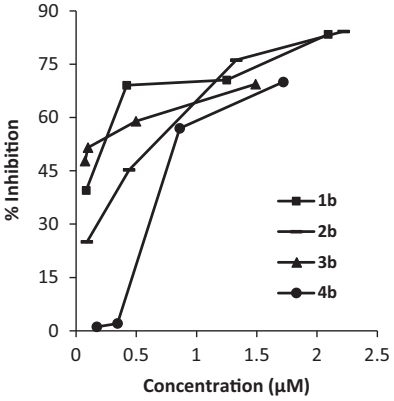

Figure 2a α-Glucosidase inhibition activity profile of Pd(II) complexes **1b–4b**.

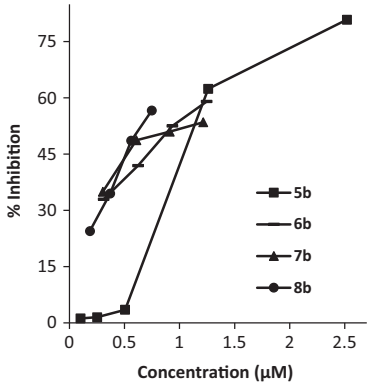

Figure 2b α-Glucosidase inhibition activity profile of Pd(II) complexes **5b–8b**.

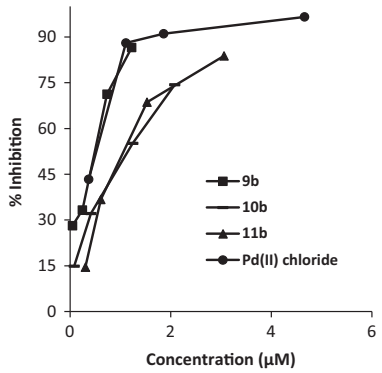

Figure 2c α-Glucosidase inhibition activity profile of Pd(II) complexes **9b–11b** and Pd(II) chloride.

complexes **1b–11b**. Every hydrazide ligand was inactive as an α-glucosidase inhibitor. Complexing the inactive ligands with Pd(II) caused a noticeable increase in the α-glucosidase inhibitory potential of ligands, highlighting the crucial role of the Pd(II) metal center during enzyme inhibition. This study predicts the dose-dependent α-glucosidase inhibition caused by the Pd(II)-hydrazide complexes; the inhibition activity increased as the concentration of compound increased in the tested range (Figs. 2a–c).

All of the Pd(II)-hydrazide complexes were highly potent α-glucosidase inhibitors (IC_{50} = 0.09–1.20 μM) and were approximately 300 times more active than the standard α-glucosidase inhibitor, DNJ (IC_{50} = 300 μM). In the literature, there are plenty of examples of metal complexes with various metal ions, which exhibit excellent α-glucosidase inhibition efficacies (Yoshikawa et al., 2010; Hiromura and Sakurai, 2008; Sakurai, 2008; Kiss et al., 2008; Ueda et al., 2005; Thompson et al., 2003). α-Glucosidase inhibition activity revealed by Pd(II)-hydrazide complexes is higher (lower IC_{50} values) than some potential antidiabetic zinc(II) complexes studied by Ueda et al., 2005.

The precursor metal salt ($PdCl_2$) was also an excellent α-glucosidase inhibitor (IC_{50} = 0.45 μM). The results of present study are in good accord with those obtained by Ueda et al., 2005 for zinc(II) complex $[Zn(6mpa\text{-}ma)_2]SO_4$. The ligand 6mpa-ma (i.e., 6-methyl-2-picolinmethylamide) was completely inactive, while the respective zinc complex was several times more efficient α-glucosidase inhibitor compared to acarbose (standard medicine), and even the metal salt ($ZnCl_2$) was almost equally potent as resulting zinc complex. The imidazole and carboxy groups have been documented earlier as most closely related active site residues of α-glucosidases (Chiba and Shimomura, 1979). The palladium(II) ion, being a soft Lewis acid, may coordinate to α-glucosidase through soft electron donors, such as imidazole nitrogen, leading to inhibition of enzyme. Cornman et al., 1995 previously suggested that forming a bond between a metal ion and a protein side chain might inhibit or activate enzymes.

The complexation of Pd(II) with inactive hydrazide ligands modified its inhibition activity. Three ligands (**1**, **3** and **9**) strengthened the Pd(II)-complexes' inhibitory effect relative to the $PdCl_2$, but eight ligands (**2**, **4–8**, **10** and **11**) decreased the inhibitory potential of $PdCl_2$ after complexation. Therefore, the inactive ligand can increase or decrease the enzyme inhibition activity of the precursor metal compound, which may be related to change in the structural or electronic properties.

The nature and position of the substituents in the Pd(II) complexes modulate the α-glucosidase inhibition. Complexes containing fluoro (**1b** and **3b**), methoxy (**6b** and **8b**) and chloro (**9b** and **11b**) substituents at the *ortho* and *para* positions are slightly stronger α-glucosidase inhibitors relative to the corresponding *meta*-substituted complexes (**2b**, **7b** and **10b**). Therefore, the Pd(II) complexes containing *meta*-substituents attached to planar phenyl ring of hydrazides may interact less favorably with α-glucosidase to inhibit the enzyme. Another interesting feature is that the electron-withdrawing fluoro- and chloro-substituted complexes (**1b–3b** and **9b–11b**) exhibit a slightly higher α-glucosidase inhibition than the electron-donating methoxy-substituted (**6b–8b**) complexes. Furthermore, the CH_2 group between the carbonyl group and the benzene ring of the hydrazide ligand in complex **5b** lowers the α-glucosidase inhibition power more than complex **4b**, which contains an NH group in place of the CH_2 group. It is therefore suggested that the presence of electron withdrawing groups or electronegative atoms (e.g., halogens or nitrogen) is responsible for greater α-glucosidase inhibition abilities of Pd(II) complexes, probably due to hydrogen bonding properties.

Zhou et al., 2006 established that the inhibitor's hydrogen bond-forming capabilities with the catalytic residue of α-glucosidase in the inhibition action are important. There are numerous hydrogen bond-donating or bond-accepting sites (NH/C=O/NH_2) on the hydrazide moiety of the Pd(II) complexes; these sites may H-bond with α-glucosidase, causing enzyme inhibition. For acarbose and acarbose-like α-glucosidase inhibitors, Park et al., 2008 revealed that the side chain of Thr 215 in α-glucosidase is a hydrogen bond acceptor and the side chain hydroxyl group on Ser244 is a hydrogen bond donor. The nature and position of the substituents on the complexed hydrazide moiety may influence the hydrogen bond-donating or bond-accepting capabilities of the Pd(II) complexes.

Therefore, the presence of Pd(II) contributes to α-glucosidase inhibition. The inhibitors may be stabilized further in the active site by hydrogen bonding with the catalytic residues and establishing cooperative hydrophobic contacts. Inhibition might be modulated by the electronic effects that depend upon the different substituents or groups in the inhibitor. Since the Pd(II) compounds show several hundred fold more α-glucosidase inhibition activity than the standard inhibitor (DNJ), such effective α-glucosidase inhibitors of synthetic origin may prove to be of importance in antidiabetic chemotherapy and related disorders in future.

Table 2 Carbonic anhydrase II inhibition activity of palladium(II) complexes.

Compound	IC_{50} (μM)	Compound	IC_{50} (μM)
1b	446.18 ± 8.27	**8b**	> 500
2b	14.43 ± 0.91	**9b**	295.04 ± 2.05
3b	56.00 ± 1.56	**10b**	10.80 ± 0.46
4b	> 500	**11b**	240.7 ± 1.15
5b	> 500	$PdCl_2$	17.34 ± 0.40
6b	17.07 ± 0.35	ACZ	0.12 ± 0.03
7b	> 500	–	–

ACZ = Acetazolamide, the standard inhibitor of carbonic anhydrase.

Table 3 Kinetics of the carbonic anhydrase II inhibition activity of palladium(II) complexes.

Sample code	[*I*] (μM)	V_{max} (μM/min)	K_m (mM)	$V_{max\ (app)}$ (μM/min)	$K_{m(app)}$ (mM)	K_i (μM)	Type of inhibition
2b	12.5	73.52	2.91	16.58	1.70	9.45	Mixed-type inhibition
6b	50	82.64	3.6	103	7.43	27.11	Mixed-type inhibition
10b	50	73.52	2.91	25.31	1.71	25.2	Mixed-type inhibition
$PdCl_2$	50	136.96	3.4	78.74	8.28	16.50	Mixed-type inhibition
ACZ	0.17	48.32	3.5	14.22	3.4	0.07	Noncompetitive

ACZ = Acetazolamide, the standard inhibitor of carbonic anhydrase.
[*I*] = Concentration of inhibitor, it is zero for columns V_{max} and K_m.
V_{max} = Maximum velocity of enzymatic activity without inhibitor.
$V_{max\ (app)}$ = Maximum velocity of enzymatic activity in the presence of inhibitor at given concentration.
K_m = Michaelis–Menten constant without inhibitor.
$K_{m(app)}$ = Michaelis–Menten constant in the presence of inhibitor at given concentration.
K_i = Inhibition constant calculated from secondary re-plot of Lineweaver–Burk plot.

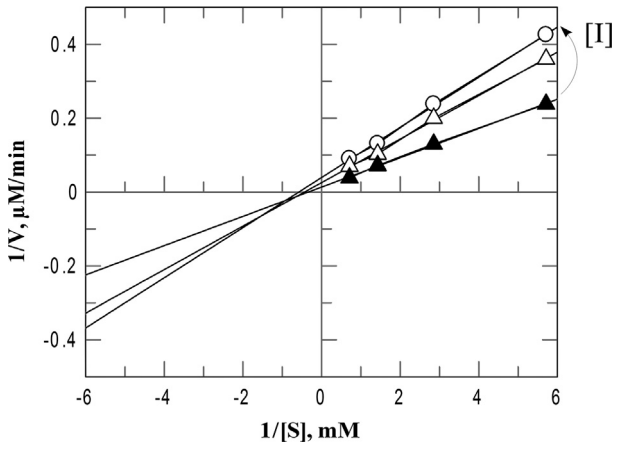

Figure 3a Kinetics of CA II inhibition by **10b**. The Lineweaver–Burk plot in the absence and presence of different concentrations of **10b** (μM): 0 (▲), 3 (Δ) and 50 (○). It indicates mixed non-competitive inhibition.

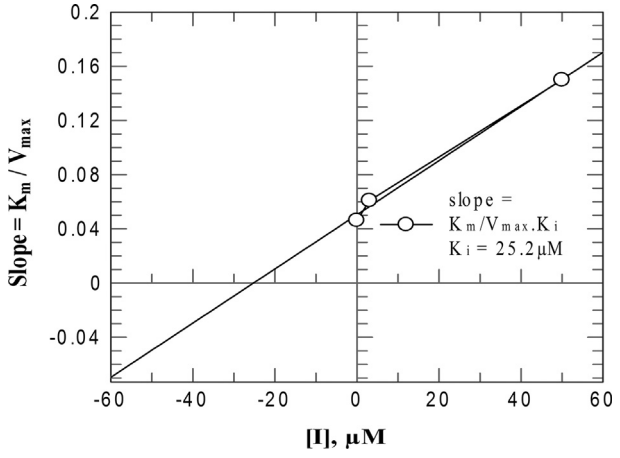

Figure 3b Kinetics of CA II inhibition by **10b**. The secondary re-plot of Lineweaver–Burk plot drawn between slope and various concentrations of **10b**. It gives inhibition constant (K_i).

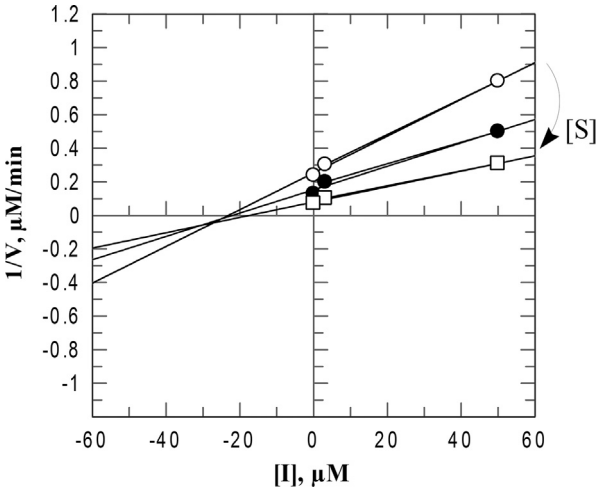

Figure 3c Kinetics of CA II inhibition by **10b**. The Dixon plot for **10b** in the presence of different concentrations of 4-NPA substrate (mM): 0.18 (○), 0.35 (●) and 0.7 (□). It confirms K_i value and mixed type non-competitive inhibition.

3.4. Carbonic anhydrase inhibition

The IC_{50} values for the inhibition of the CA-II enzyme by palladium complexes are presented in Table 2. After screening synthesized palladium metal complexes against CA, only a few complexes revealed excellent inhibition, where the IC_{50} values ranged from 10.80 to 446.18 μM. Compounds **2b**, **6b** and **10b** were excellent inhibitors compared to a palladium salt. The other compounds displayed weak inhibition.

The metal salt and its three complexes (**2b**, **6b** and **10b**) were subjected to kinetics-based mechanistic studies to identify the type of inhibition (Table 3). Determining the type of inhibition is very important for identifying the inhibition mechanism and interactions of the ligands with the enzymatic active site. The graphical analysis of the steady state inhibition data for **10b** against carbonic anhydrase is presented in Figs. 3a–3c. The Lineweaver–Burk plot identifies that all tested compounds exhibit a mixed type non-competitive inhibition of CA II with 4-NPA (substrate) since both V_{max} and K_m values are changed (having an intersecting point) during the enzymatic reaction in the presence of inhibitor (Dixon, 1953). Using

Lineweaver–Burk plot, the values of K_m (without inhibitor) and $K_{m(app)}$ (in the presence of inhibitor) were obtained from the intersection of abscissa, while $1/V_{max}$ (without inhibitor) and $1/V_{max(app)}$ (in the presence of inhibitor) were obtained from the intersection of ordinate. The secondary re-plot of Lineweaver–Burk plot between slope ($=K_m/V_{max}$) and inhibitor concentration gives inhibition or dissociation constant (K_i). The larger K_i value reflects weaker binding of inhibitor to CA II. The Dixon plot further confirms the K_i value and existence of mixed type inhibition; the intersection point is not exactly on [*I*] axis but nearer to *x*-axis in the Dixon plot, excluding the presence of pure non-competitive inhibition (Dixon, 1953; Cornish-Bowden, 1974). The mixed inhibition dictates the binding of Pd(II) compounds at a site other than the substrate binding site in the active site cavity of CA II; for example, Pd(II) may easily interact with sulfur or nitrogen donor amino acids to inhibit the enzyme, similar to metal complexes of sulfonamides (Briganti et al., 1997). In addition, a Pd(II)-based CAI may bind both free enzyme and enzyme-substrate (ES) complex, but having different affinity for one state or the other (Storey, 2004). Lineweaver–Burk plot and Table 3 illustrate that in case of $PdCl_2$ and **6b**, there is a decrease in the apparent affinity of the enzyme for the substrate ($K_{m(app)} > K_m$), i.e., an increase in K_m value in the presence of inhibitor, showing that the $PdCl_2$ and **6b** favor binding the free enzyme. In contrast, the compounds **2b** and **10b** show an increase in the apparent affinity for the substrate ($K_{m(app)} < K_m$), i.e., a decrease in the K_m value in the presence of inhibitor, indicating that these two inhibitors preferably bind to ES complex (Storey, 2004).

The hydrazide ligands (**1–11**) exhibited no inhibition against carbonic anhydrase. In contrast, the Pd(II) hydrazide complexes revealed varied IC_{50} values (Table 2), indicating excellent, moderate, and weak inhibition of carbonic anhydrase. These results were consistent with previous studies describing CA inhibition caused by various metal (Zn^{2+}, Cd^{2+}, Hg^{2+}, Co^{2+}, Ni^{2+}, Cu^{2+}, V^{4+}, Fe^{3+}, Ag^{+}, Be^{2+}, Mg^{2+}, and Al^{3+}) complexes; all the metal complexes were stronger inhibitors of CA relative to their parent ligands (Scozzafava and Supuran, 1997; Supuran et al., 1997).

The precursor metal salt ($PdCl_2$) is also a good CA inhibitor (IC_{50} = 17.34 μM); however the complexation of the hydrazide ligands with 3-fluoro (**2**), 2-methoxy (**6**) and 3-chloro (**10**) substituents with Pd(II) further enhanced inhibitory potential for their complexes (**2b**, **6b** and **10b**) relative to the precursor metal; these CA inhibitors had IC_{50} values of 14.43, 17.07 and 10.80 μM, respectively. These IC_{50} values were comparable to the standard inhibitor, ACZ (IC_{50} = 0.12 μM). Complex **3b**, which contained a 4-fluoro group on the benzene ring of its hydrazide moiety, moderately inhibited CA (IC_{50} = 56 μM), while **1b**, **9b** and **11b** (2-fluoro, 2-chloro and 4-chloro substituents, respectively) exhibited weak inhibition (IC_{50} = 446.18, 295.04 and 240.7 μM, respectively). The remaining four complexes, **4b** (NH group between benzene ring and carbonyl groups), **5b** (CH_2 group between benzene ring and carbonyl groups), **7b** (3-methoxy substituent) and **8b** (4-methoxy substituent) were poor CA inhibitors with IC_{50} values above 500 μM.

The results demonstrate that the presence of fluoro (**1b–3b**) and chloro (**9b–11b**) substituents plays important role in presenting CA inhibition properties to Pd(II) complexes. The halo groups may contribute in the polarizability of the complexes that would make it possible for halo complexes to interact with the hydrophilic patch situated at the entrance of CA II active site (Briganti et al., 1997).

The mechanism for carbonic anhydrase inhibition by the metal complexes relative to their parent ligands is currently unknown, but it has been hypothesized that their enhanced inhibitory potential might be caused by two phenomena that occur separately or in concert: (i) the dissociation of a metal complex inhibitor to form hydrazides and Pd(II) ions (in diluted solution), which allows both species to interact with their respective binding sites and (ii) the direct interaction between the undissociated Pd(II) complex and the enzyme, specifically the hydrophilic portion near the entrance of the CA II active sites (Briganti et al., 1997). In present case, since the ligands themselves are inactive to inhibit the enzyme, it is suggested that the later mechanism is more favorable to occur, and the undissociated Pd(II)-hydrazide complex might be the CA II inhibitory species. The similar mechanism to bind CA I has previously been proposed by Borras et al. (1996) for Ni(II) complexes of sulfonamides and hydrazine. Since kinetic studies reveal mixed non-competitive inhibition, it is presumed that the Pd(II) ion in the undissociated complex would interact with histidine residues, especially the imidazole ring of His 64 (a proton shuttle group that has been described as a favorable metal interaction site) (Magerum and Dukes, 1974; Steiner et al., 1975). These considerations are in accord with studies reported by Briganti et al. (1997) and Elbaum et al. (1996) for metal complexes of sulfonamides. The chance of direct coordination of hydrazide ligands to zinc(II) active site may be ruled out because the observed mechanism is a non-competitive type. However, there is a great possibility that the ligand may involve in hydrogen bonding interactions through its NH or carbonyl group with Thr199 residue present in the hydrophobic cavity, similar to nitrate, cyanide and cyanates (Liljas et al., 1994). Further research is necessary to elucidate the actual mechanism of CA inhibition utilized by the Pd(II) complexes and to develop Pd(II)-based diuretic, antiglaucoma, antiobesity, antiulcer and/or anti-infective drugs.

4. Conclusions

We developed a series of Pd(II) hydrazide complexes that were characterized using physical, chemical and spectral measurements; these complexes exhibited a square planar geometry and the general formula $[PdL_2Cl_2]$. Each of the Pd(II) complexes demonstrated several hundred-fold higher α-glucosidase inhibition activity than the standard inhibitor, 1-deoxynojirimycin. The development of effective synthetic α-glucosidase inhibitors may prove important for anti-diabetic chemotherapy and treatments for other related disorders. Some of the Pd(II) complexes are also excellent carbonic anhydrase inhibitors, making them interesting anti-glaucoma drug candidates.

Acknowledgments

We thank the *Higher Education Commission of Pakistan* for financial support ('The National Research Grants Program for Universities', grant No.1862/R&D/10) and MMT acknowledges the support from Fulbright Scholar Award from The J. William Fulbright Foreign Scholarship Board.

Appendix A. Supplementary material

Supplementary data associated with this article can be found, in the online version, at http://dx.doi.org/10.1016/j.arabjc.2015.02.024.

References

Abdul, A.H.K., Abu, B.M., Al-Amiery, A.A., Takriff, M.S., 2011. Antimicrobial and antioxidant activities of new metal complexes derived from 3-aminocoumarin. Molecules 16, 6969–6984.

Abu-Surrah, A.S., Al-Allaf, T.A., Rashan, L.J., Klinga, M., Leskelä, M., 2002. Synthesis, crystal structure and initial biological evaluation of new enantiomerically pure chiral palladium(II) complex trans-bis[endo-(1R)-1,7,7-trimethylbicyclo[2.2.1]-heptan-2-amino]palladium(II) dichloride. Eur. J. Med. Chem. 37, 919–922.

Adeoye, I.O., Adelowo, O.O., Oladip, M.H., Odunola, O.A., 2007. Comparison of bactericidal and fungicidal activities of Cu(II) and Ni(II) complexes of para-methoxy- and para-hydroxybenzoic acid hydrazide. Res. J. Appl. Sci. 2, 590–594.

Ara, R., Ashiq, U., Mahroof-Tahir, M., Maqsood, Z.T., Khan, K.M., Lodhi, M.A., Choudhary, M.I., 2007. Chemistry, urease inhibition, and phytotoxic studies of binuclear vanadium (IV) complexes. Chem. Biodivers. 4, 58–71.

Arslan, O., 2001. Inhibition of bovine carbonic anhydrase by new sulfonamide compounds. Biochemistry (Mosc) 66, 982–983.

Ashiq, U., Ara, R., Mahroof-Tahir, M., Maqsood, Z.T., Khan, K.M., Khan, S.N., Siddiqui, H., Choudhary, M.I., 2008. Synthesis, spectroscopy, and biological properties of vanadium(IV)-hydrazide complexes. Chem. Biodivers. 5, 82–92.

Ashiq, U., Ara, R., Mahroof-Tahir, M., Maqsood, Z.T., Khan, K.M., Omer, I., Choudhary, M.I., 2009. Studies of enzyme inhibition, radical scavanging and spectroscopic studies of vanadium(IV)-hydrazide complexes. J. Enz. Inhibit. Med. Chem. 24, 1336–1343.

Atta-ur-Rahman, Choudhary, M.I., Basha, F.Z., Abbas, G., Khan, S.N., Ali, S.S.A., 2007. Science at the interface of chemistry and biology: discoveries of α-glucosidase inhibitors and antiglycation agents. Pure Appl. Chem. 79, 2263–2268.

Ballhausen, C.J., Gray, H.B., 1962. The electronic structure of vanadyl ion. Inorg. Chem. 1, 111–122.

Basu, B.S., Basu, B.T.S., Rivarola, E., 1999. Organotin(IV) complexes of aromatic acid hydrazides: Preparation and spectroscopic studies. Synth. React. Inorg. Met.-Org. Chem. 29, 215–231.

Blanchard, S., Neese, F., Bothe, E., Bill, E., Weyhermüller, T., Wieghardt, K., 2005. Square planar vs. tetrahedral coordination in diamagnetic complexes of nickel(II) containing two bidentate pi-radical monoanions. Inorg. Chem. 44, 3636–3656.

Borras, J., Casanova, J., Cristea, T., Gheorghe, A., Scozzafava, A., Supuran, C.T., Tudor, V., 1996. Complexes with biologically active ligands. Part 6-Ni(II) coordination compounds of hydrazine and heterocyclic sulfonamides as inhibitors of the zinc enzyme carbonic anhydrase. Met. Based Drugs 3, 143–148.

Braun, C., Brayer, G.D., Withers, S.G., 1995. Mechanism-based inhibition of yeast alpha-glucosidase and human pancreatic alpha-amylase by a new class of inhibitors: 2-deoxy-2,2-difluoro alpha-glycosides. J. Biol. Chem. 270, 26778–26781.

Briganti, F., Mangani, S., Orioli, P., Scozzafava, A., Vernaglione, G., Supuran, C.T., 1997. Carbonic anhydrase activators: X-ray crystallographic and spectroscopic investigations for the interaction of isozymes I and II with histamine. Biochemistry 36, 10384–10392.

Carroll, M.F., Gutierrez, A., Castro, M., Tsewang, D., Schade, D.S., 2003. Targeting postprandial hyperglycemia: a comparative study of insulinotropic agents in type 2 diabetes. J. Clin. Endocrinol. Metab. 88, 5248–5254.

Chiasson, J.L., Rabasa Lhoret, R., 2004. Prevention of Type 2 Diabetes: insulin resistance and B-cell function. Diabetes 53, S34–S38.

Chiba, S., 1997. Molecular mechanism in α-glucosidase and glucoamylase. Bio. Sci. Biotech. Biochem. 61, 1233–1239.

Chiba, S., Shimomura, T., 1979. Transglucosylation of α-glucosidase. J. Jpn. Soc. Starch. Sci. 26, 59–67.

Chohan, Z.H., Hanif, M., 2011. Synthesis and characterization of biologically active new Schiff bases containing 3-functionalized 1,2,4-triazoles and their zinc(II) complexes: crystal structure of 4-bromo-2-[(E)-(1H-1,2,4-triazol-3-ylimino)-methyl]phenol. Appl. Organomet. Chem. 25, 753–760.

Chohan, Z.H., Praveen, M., 1999. Synthesis, spectroscopic and biological studies of some mono- and di-substituted hydrazine-derived ferrocenes. Pak. J. Pharmaceut. Sci. 12, 1–6.

Cornish-Bowden, A., 1974. A simple graphical method for determining the inhibition constants of mixed, uncompetitive and non-competitive inhibitors. Biochem. J. 137, 143–144.

Cornman, C.R., Zovinka, E.P., Meixner, M.H., 1995. Vanadium complexes of the active-site peptide of protein tyrosine phosphatase. Inorg. Chem. 34, 5099–5100.

Coulston, L., Dandona, P., 1980. Insulin-like effect of zinc on adipocytes. Diabetes 29, 665–667.

Dewi, R.T., Iskandar, Y.M., Hanafi, M., Kardono, L.B.S., Angelina, M., Dewijanti, I.D., Banjarnahor, S.D., 2007. Inhibitory effect of koji Aspergillus terreus on alpha-glucosidase activity and post-prandial hyperglycemia. Pak. J. Biol. Sci. 10, 3131–3135.

Dixon, M., 1953. The determination of enzyme inhibitor constants. Biochem. J. 55, 170–171.

Dwek, R.A., Butters, T.D., Platt, F.M., Zitzmann, N., 2002. Targeting glycosylation as a therapeutic approach. Nat. Rev. Drug Discov. 1, 65–75.

Ebbing, D., Steven, D.G., 2010. General Chemistry Enhanced Edition, ninth ed. Cengage Learning Inc., Florence.

Elbaum, D., Nair, S.K., Patchan, M.W., Thompson, R.B., Christianson, D.W., 1996. Structure-based design of a sulfonamide probe for fluorescence anisotropy detection of zinc with a carbonic anhydrase-based biosensor. J. Am. Chem. Soc. 118, 8381–8387.

Franco, O.L., Rigden, D.J., Melo, F.R., Grosside-Sa, M.F., 2002. Plant α-amylase inhibitors and their interaction with insect α-amylases. Eur. J. Biochem. 269, 397–412.

Funke, I., Melzig, M.F., 2006. Traditionally used plants in diabetes therapy. Phytotherapeutics as inhibitors of α-amylase activity. Revista Brasileira de Farmacognosia/Brazil. J. Pharm. 16, 1–5.

Heyliger, C.E., Tahiliani, A.G., McNeill, J.H., 1985. Effect of vanadate on elevated blood glucose and depressed cardiac performance of diabetic rats. Science 227, 1474–1476.

Hiromura, M., Sakurai, H., 2008. Action mechanism of insulin-mimetic vanadyl-allixin complex. Chem. Biodivers. 5, 1615–1621.

Ho, Y.T., Purohit, A., Vicker, N., Newman, S.A.P., Robinson, J.J., Leese, M.P., Ganesshapillai, D., Woo, L.W.L., Reed, M., 2003. Inhibition of carbonic anhydrase II by steroidal and non-steroidal sulphamates. J. Biochem. Biophys. Res. Commun. 305, 909–914.

Jaiswal, N., Srivastava, S.P., Bhatia, V., Mishra, A., Sonkar, A.K., Narender, T., Srivastava, A.K., 2012. Inhibition of alpha-glucosidase by Acacia nilotica prevents hyperglycemia along with improvement of diabetic complications via aldose reductase inhibition. J. Diabetes Metab. 6, 1–7.

Karpas, A., Fleet, G.W., Dwek, R.A., Petursson, S., Namgoong, S.K., Ramsden, N.G., Jacob, G.S., Rademacher, T.W., 1988. Aminosugar derivatives as potential anti-human immunodeficiency virus agents. Proc. Natl. Acad. Sci. USA 85, 9229–9233.

Kealey, S., Long, N.J., Miller, P.W., White, A.J., Hitchcock, P.B., Gee, A., 2007. Variable coordination behaviour of pyrazole-containing N, P and N, P(O) ligands towards palladium(II). Dalton Trans. 26, 2823–2832.

Kim, K.Y., Nam, K.A., Kurihara, H., Kim, S.M., 2008. Potent α-glucosidase inhibitors purified from the red alga *Grateloupia elliptica*. Phytochemistry 69, 2820–2825.

Kiss, T., Jakusch, T., Hollender, D., Dornyei, A., Enyedy, E.A., Pessoa, J.C., Sakurai, H., Sanz-Medel, A., 2008. Biospeciation of

antidiabetic VO(IV) complexes. Coord. Chem. Rev. 252, 1153–1162.
Kucukguzel, S.G., Mazi, A., Sahin, F., Ozturk, S., Stables, J., 2003. Synthesis and biological activities of diflunisal hydrazide-hydrazones. Eur. J. Med. Chem. 38, 1005–1013.
Kuznetsov, V.V., Skibina, L.M., Khalikov, R.R., 2006. Effect of the structure of benzohydrazides on cadmium electrodeposition from perchlorate and iodide electrolytes. Prot. Met 42, 570–576.
Lajolo, F.M., Filho, J.M., Menezes, E.W., 1984. Effect of a bean (*Phaseolus vulgaris*, L.) alfa-amylase inhibitor on starch utilization. Nutr. Rep. Int. 30, 45–54.
Liljas, A., Hfkansson, K., Harald, B., Jonsson, B.H., Xue, Y., 1994. Inhibition and catalysis of carbonic anhydrase. Recent crystallographic analyses. Eur. J. Biochem. 219, 1–10.
Lubna, S.M., Isam, S.H., Falah, R.M., Bahjat, R.J., 2014. DFT and MP2 study of Pd(II) and Ni(II) PhCN, DMSO and dithiooxamide complexes- Part II: Theoretical. J. Appl. Chem. 3, 2102–2122.
Madariaga, H., Lee, P.C., Heitlinger, L.A., Lenenthal, M., 1988. Effects of graded alpha-glucosidase inhibition on sugar absorption *in vivo*. Dig. Dis. Sci. 33, 1020–1024.
Magerum, D.W., Dukes, G.R., 1974. In: Metal Ions in Biological Systems, vol. 1. Marcel Dekker, New York.
Maqsood, Z.T., Khan, K.M., Ashiq, U., Jamal, R.A., Chohan, Z.H., Mahroof- Tahir, M., Supuran, C.T., 2006. Oxovanadium (IV) complex of hydrazides: potential antifungal agents. J. Enzym. Inhib. Med. Chem. 21, 37–42.
McCulloch, D.K., Kurtz, A.B., Tattersall, R.B., 1983. A new approach to the treatment of nocturnal hypoglycemia using alpha-glucosidase inhibition. Diabetes Care 6, 483–487.
Mehta, A., Zitzmann, N., Rudd, P.M., Block, T.M., Dwek, R.A., 1998. Alpha-glucosidase inhibitors as potential broad based antiviral agents. FEBS Lett. 430, 17–22.
Mirshafiey, A., Boghozian, R., 2011. In: Atta-ur-Rahman, Choudhary, M.I. (Eds.), Anti-angiogenesis Drug Discovery and Development. Bentham Science Publishers Ltd.
Mishra, A.P., Soni, M., 2008. Synthesis, structural, and biological studies of some Schiff bases and their metal complexes. Met. Based Drug. 2008, 1–7.
Mukherjee, S., Gangopadhyay, S., Zangrando, E., Gangopadhyay, P.K., 2011. Synthesis, characterization and structures of nickel(II) and palladium(II) complexes of aromatic thiohydrazides. J. Coord. Chem. 64, 3700–3710.
Muralidhara, R.B., Narayana, B., Mathew, B., Subrahmanya, B., 1995. Indirect complexometric determination of palladium(II) using sodium nitrite as a selective masking reagent. Mikrochim. Acta 118, 63–68.
Abd El Wahed, M.G., Wanees, A.E., El Gamel, M., Abd El Haleem, S., 2004. Physico-chemical studies of some aminobenzoic acid hydrazide complexes. J. Serb. Chem. Soc. 69, 255–264.
Park, H., Hwang, K.Y., Kim, Y.H., Oh, K.H., Lee, J.Y., Kim, K., 2008. Discovery and biological evaluation of novel α-glucosidase inhibitors with in vivo antidiabetic effect. Bioorg. Med. Chem. Lett. 18, 3711–3715.
Pavia, D.L., Lampman, G.M., Kriz, G.S., 2001. Introduction to Spectroscopy, third ed. Harcourt College Publishers Fort Worth, New York.
Piotr, D., Anna, B., Maria, K., Tadeusz, L., 2005. Synthesis, structure and vibrational spectroscopy of palladium(II) complexes with 2-thiophenecarboxylic hydrazide (tch). Vib. Spect. 40, 118–126.
Pocker, Y., Meany, J.E., 1967. The catalytic versatility of erythrocyte carbonic anhydrase. II. Kinetic studies of the enzyme-catalyzed hydration of pyridine aldehydes. Biochemistry 6, 239–249.
Pradeep, K., Balasubramanian, N., Deepika, S., 2008. Substituted benzoic acid benzylidene/furan-2-yl-methylene hydrazides: synthesis, antimicrobial evaluation and QSAR analysis. Arkivoc 13, 159–178.
Qurrat-ul-Ain, Ashiq, U., Jamal, R.A., Mahrooof-Tahir, M., 2013. Synthesis, spectroscopic and radical scavenging studies of palladium(II)-hydrazide complexes. Spectrochim. Acta A Mol. Biomol. Spectrosc. 115, 683–689.
Rubenstein, A.H., Levin, N.W., Elliott, G.A., 1962. Hypoglycæmia induced by manganese. Nature 194, 188–189.
Sakurai, H., 2008. Treatment of diabetes in experimental animals by metallocomplexes. Yakugaku Zasshi 128, 317–322.
Sakurai, H., Tsuchiya, K., Nukatsuka, M., Sofue, M., Kawada, J., 1990. Insulin-like effect of vanadyl ion on streptozotocin-induced diabetic rats. J. Endocrinol. 126, 451–459.
Schwarz, K., Mertz, W., 1959. Chromium(III) and the glucose tolerance factor. Arch. Biochem. Biophys. 85, 292–295.
Scozzafava, A., Supuran, C.T., 1997. Complexes with biologically active ligands. Part 101 Inhibition of carbonic anhydrase isozymes I and II with metal complexes of imidazole[2,1-b]-1,3,4-thiadiazole-2-sulfonamide. Met. Based Drugs 4, 19–26.
Shank, R.P., Doose, D.R., Streeter, A.J., Bialer, M., 2005. Plasma and whole blood pharmacokinetics of topiramate: the role of carbonic anhydrase. Epilepsy Res. 63, 103–112.
Sharma, M.C., Sahu, N.K., Kohli, D.V., Chaturvedi, S.C., Sharma, S., 2009. Molecular modelling studies of some substituted 2-butylbenzimidazoles angiotensin II receptor antagonists as antihypertensive agents. Dig. J. Nanomat. Biostruct. 4, 843–856.
Si, M.M., Lou, J.S., Zhou, C.X., Shen, J.N., Wu, H.H., Yang, B., He, Q.J., Wu, H.S., 2010. Insulin releasing and alpha-glucosidase inhibitory activity of ethyl acetate fraction of *Acorus calamus* in vitro and in vivo. J. Ethnopharmacol. 128, 154–159.
Singh, R.V., Fahmi, N., Biyala, M.K., 2005. Coordination behavior and biopotency of N and S/O donor ligands with their palladium(II) and platinum(II) complexes. J. Iran. Chem. Soc. 2, 40–46.
Slama, G., Elgrably, F., Sola, A., Mbemba, J., Larger, E., 2006. Postprandial glycaemia: a plea for the frequent use of delta postprandial glycaemia in the treatment of diabetic patients. Diabetes Metab. 32, 187–192.
Sou, S., Takahash, i H., Yamasaki, R., Kagechika, H., Endo, Y., Hashimoto, Y., 2001. Alpha-glucosidase inhibitors with a 4,5,6,7-tetrachlorophthalimide skeleton pendanted with a cycloalkyl or dicarba-closo-dodecaborane group. Chem. Pharm. Bull. 49, 791–793.
Srianta, I., Kusumawati, N., Nugerahani, I., Artanti, N., Xu, G.R., 2013. In vitro α-glucosidase inhibitory activity of Monascus-fermented durian seed extracts. Int. Food Res. J. 20, 533–536.
Steiner, H., Jonsson, B.H., Lindskog, S., 1975. The catalytic mechanism of carbonic anhydrase. Eur. J. Biochem. 59, 253–259.
Storey, K.B., 2004. Functional Metabolism: Regulation and Adaptation, first ed. Wiley-Liss, New York.
Sunirban, D., Samudranil, P., 2006. Synthesis, characterization and structural studies of palladium(II) complexes with *N*-(aroyl)-*N*′-(2,4-dimethoxybenzylidene)hydrazines. J. Organomet. Chem. 691, 2575–2583.
Supuran, C.T., Scozzafava, A., 2000. Carbonic anhydrase inhibitors and their therapeutic potential. Expert Opin. Ther. Pat. 10, 575–600.
Supuran, C.T., Scozzafava, A., Jitianu, A., 1997. Carbonic anhydrase inhibitors. Part 541: Metal complexes of heterocyclic sulfonamides: a new class of antiglaucoma agents. Met. Based Drugs 4, 307–315.
Supuran, C.T., Scozzafava, A., Casini, A., 2003. Carbonic anhydrase inhibitors. Med. Res. Rev. 23, 146–189.
Supuran, C.T., Scozzafava, A., Conway, J., 2004. Carbonic Anhydrase: Its Inhibitors and Activators. CRC Press, Boca Raton.
Teotia, M.P., Rastogi, D.K., Malik, W.U., 1973. Stereochemical features vis-à-vis spectral data on some Ni(II) complexes with coumarin derivatives. Inorg. Chim. Acta 7, 339–344.
Thompson, K.H., Liboiron, B.D., Sun, Y., Bellman, K., Setyawati, I.A., Patrick, B.O., Karunaratne, V., Rawji, G., Wheeler, J., Sutton, K., Bhanot, S., Cassidy, C., McNeill, J.H., Yuen, V.G., Orvig, C., 2003. Preparation and characterization of vanadyl complexes with bidentate maltol-type ligands; in vivo comparisons

of anti-diabetic therapeutic potential. J. Biol. Inorg. Chem. 8, 66–74.

Tripp, B.C., Smith, K., Ferry, G.M., 2001. Carbonic anhydrase: new insights for an ancient enzyme. J. Biol. Chem. 276, 48615–48618.

Truscheit, E., Frommer, W., Junge, B., Müller, L., Schmidt, D.D., Wingender, W., 1981. Chemistry and biochemistry of microbial α-glucosidase inhibitors. Angew. Chem. Int. Ed. Engl. 20, 744–761.

Ueda, E., Yoshikawa, Y., Sakurai, H., Kojima, Y., Kajiwara, M.N., 2005. *In vitro* alpha-glucosidase inhibitory effect of Zn(II) complex with 6-methyl-2-picolinmethylamide. Chem. Pharm. Bull. 53, 451–452.

Yoshikawa, Y., Ueda, E., Kawabe, K., Miyake, H., Sakurai, H., Kojima, Y., 2000. New insulin-mimetic zinc(II) complexes; bis-maltolato zinc(II) and bis-2-hydroxypyridine-N-oxide zinc(II) with Zn(O-4) coordination mode. Chem. Lett. 29, 874–875.

Yoshikawa, Y., Hirata, R., Yasui, H., Hattori, M., Sakurai, H., 2010. Inhibitory effect of $CuSO_4$ on α-glucosidase activity in ddY mice. Metallomics 2, 67–73.

Zhdanov, Y.A., Minkin, V.I., 1966. Correlation Analysis in Organic Chemistry. Rostov Univ, Rostov-on-Don.

Zhou, J.M., Zhou, J.H., Meng, Y., Chen, M.B., 2006. Molecular dynamics simulation of iminosugar inhibitor-glycosidase complex: Insight into the binding mechanism of 1-deoxynojirimycin and isofagomine toward β-glucosidase. J. Chem. Theory Comput. 2, 157–165.

Ziolo, R.F., Gaughan, A.P., Dori, Z., Pierpont, C.G., Eisenberg, R., 1971. The crystal and molecular structure of p-diazido-tetrakis(tripheny1phosphine)dicdpper(I). Inorg. Chem. 10, 1289–1296.

Zitzmann, N., Mehta, A.S., Carrouée, S., Butters, T.D., Platt, F.M., McCauley, J., Blumberg, B.S., Dwek, R.A., Block, T.M., 1999. Imino sugars inhibit the formation and secretion of bovine viral diarrhea virus, a pestivirus model of hepatitis C virus: implications for the development of broad spectrum anti-hepatitis virus agents. Proc. Natl. Acad. Sci. USA 96, 11878–11882.